

Plumboferrite: New mineralogical data and atomic arrangement

DAN HOLTSTAM*

Institute of Earth Sciences, Uppsala University, Norbyvägen 18 B, S-752 36 Uppsala, Sweden

ROLF NORRESTAM, ARNE SJÖDIN

Department of Structural Chemistry, Arrhenius Laboratory, Stockholm University, S-106 91 Stockholm, Sweden

ABSTRACT

Plumboferrite from the type locality at Jakobsberg, Filipstad, Sweden, has been reexamined. It occurs in assemblages confined to bands in metamorphic carbonate rock and is associated with hematite, magnesioferrite-jacobsite-magnetite solid solutions, lindqvistite, calcite, andradite, phlogopite, hedyphane, svabite, hematophanite, native copper, and cuprite. Six samples investigated fall in a narrow composition range: PbO 33.9–34.6, Sb₂O₃ 0.0–0.3, Fe₂O₃ 62.4–63.9, MnO 0.6–1.8, TiO₂ 0.1–0.5, SiO₂ 0.0–0.2, Al₂O₃ 0.0–0.1, MgO 0.1–0.4 (weight percent). The mineral is moderately anisotropic and optically uniaxial (–). Reflectance values obtained in air are 25.6–24.2% (470 nm), 24.5–23.5% (546 nm), 23.7–22.8 (589 nm), and 22.6–22.1% (650 nm). $VHN_{100} = 882$ and $D_{\text{calc}} = 6.12(1)$ g/cm³.

Single-crystal X-ray studies show that plumboferrite is hexagonal, essentially $P6_3/mmc$, with the cell dimensions $a = 5.931(1)$, $c = 23.551(2)$ Å, and $V = 717.4(2)$ Å³ (refined from powder data). Overexposed precession X-ray photographs indicate the presence of a supercell with $a' = \sqrt{3}a = 10.27$ Å and $c' = 3c = 70.7$ Å (hexagonal setting). The structure of plumboferrite has been refined from the 394 most significant ($I > 5\sigma_I$) X-ray reflections with $(\sin \theta)/\lambda \leq 0.81$ Å⁻¹ to $R = 3.9\%$. It has a defect magnetoplumbite-type structure that can be described in terms of two basic structural units, the R and the S (spinel) blocks. The stacking sequence of such blocks along c is RSR'S', where ideally $R = (\text{Pb}_2\text{Fe}_3\text{O}_{11-s})$ and $S = (\text{Fe}_6\text{O}_8)$ for plumboferrite. The formula (with $Z = 2$ for the subcell) for the investigated material approaches $\text{Pb}_2\text{Me}_{0.33}\text{Fe}_{10.67}\text{O}_{18.33}$, with $\text{Me} = \text{Mn}^{2+}$, Mg, rather than PbFe_4O_7 , which is still prevalent in the literature. The departure from stoichiometry (19 O atoms per formula unit) reflects partially occupied O3 positions in the R blocks. The weak superlattice reflections observed (not included in the present refinements) probably result from the ordering of split Pb positions, O vacancies, or both.

INTRODUCTION

Plumboferrite, from the Jakobsberg deposit, Filipstad, Värmland, central Sweden, was first discovered and characterized by Igelström (1881) as an oxide of mainly Pb and Fe. A more detailed investigation of the mineral was undertaken by Johansson (1928). He arrived at PbFe_4O_7 , as the most likely composition, and it still remains the accepted formula in mineralogical handbooks (e.g., Fleischer and Mandarino, 1991). Using Laue and rotation photographs, Johansson (1928) stated that the mineral was trigonal, space group $P312$, and calculated the (hexagonal) cell parameters as $a = 11.86$ and $c = 47.14$ Å from powder data. Kohn et al. (1968) performed further X-ray single-crystal studies on plumboferrite. Their material showed a pronounced hexagonal cell with $a = 5.90$ and $c = 23.56$ Å, with probable space group $P6_3/mmc$. In addition, weak reflections indicated a rhombohedral supercell with $a' = \sqrt{3}a$ and $c' = 3c$. Its relation to mag-

netoplumbite, ideally $\text{PbFe}_{12}\text{O}_{19}$, was recognized from similarities in unit-cell geometry and composition.

In the course of a study of the natural hexagonal ferrites we have reinvestigated plumboferrite. Six samples, representative of the plumboferrite specimens in the collections of the Swedish Museum of Natural History (NRM), and including Igelström's original material (NRM no. 81: 0224), have been carefully examined.

OCCURRENCE AND MINERAL ASSEMBLAGE

The type locality of plumboferrite is one of the so-called Långban-type Fe-Mn deposits (Moore, 1970), which are characterized by an unusual enrichment of elements such as Pb, Ba, As, and Sb. The ores of the small mines of Jakobsberg constitute separate hausmannite and magnetite-hematite bodies accompanied by characteristic skarn masses (Magnusson, 1929). The mineralizations are hosted by a dolomitic marble that belongs to a rock sequence of Paleoproterozoic age, dominated by felsic metavolcanites. The supracrustal units of the Filipstad area have been affected by regional metamorphism in the amphibolite facies, followed by intrusive events, in connec-

* Present address: Department of Mineralogy, Swedish Museum of Natural History, Box 50007, S-104 05 Stockholm, Sweden.

TABLE 1. Chemical composition of plumboferrite

| Sample | 81:0224 | 280186 | 331072 | 670322 | 920741 | g7776 |
|--------------------------------|---------|--------|--------|--------|--------|-------|
| Oxide wt% | | | | | | |
| PbO | 34.18 | 34.22 | 34.34 | 34.60 | 33.94 | 33.99 |
| Sb ₂ O ₅ | 0.00 | 0.00 | 0.02 | 0.00 | 0.02 | 0.34 |
| Fe ₂ O ₃ | 63.91 | 63.28 | 63.43 | 63.82 | 62.95 | 62.36 |
| MnO | 1.24 | 1.49 | 1.62 | 0.64 | 1.79 | 1.66 |
| TiO ₂ | 0.21 | 0.17 | 0.10 | 0.12 | 0.42 | 0.53 |
| SiO ₂ | 0.10 | 0.04 | 0.17 | 0.02 | 0.13 | 0.04 |
| Al ₂ O ₃ | 0.01 | 0.07 | 0.02 | 0.02 | 0.02 | 0.02 |
| MgO | 0.29 | 0.22 | 0.11 | 0.44 | 0.17 | 0.45 |
| Total | 99.94 | 99.49 | 99.81 | 99.66 | 99.44 | 99.39 |
| 13 cations | | | | | | |
| Pb | 2.03 | 2.04 | 2.04 | 2.06 | 2.02 | 2.02 |
| Sb | 0.00 | 0.00 | 0.00 | 0.00 | 0.00 | 0.03 |
| Fe | 10.59 | 10.55 | 10.55 | 10.64 | 10.48 | 10.39 |
| Mn | 0.23 | 0.28 | 0.30 | 0.12 | 0.34 | 0.31 |
| Ti | 0.03 | 0.03 | 0.02 | 0.02 | 0.07 | 0.09 |
| Si | 0.02 | 0.01 | 0.04 | 0.00 | 0.03 | 0.01 |
| Al | 0.00 | 0.02 | 0.01 | 0.01 | 0.00 | 0.00 |
| Mg | 0.10 | 0.07 | 0.04 | 0.15 | 0.06 | 0.15 |
| O | 18.35 | 18.33 | 18.34 | 18.35 | 18.34 | 18.34 |

tion with the Svecofennian orogeny around 1.85 Ga (Björk, 1986).

Plumboferrite is locally abundant at Jakobsberg and occurs in oxide mineral assemblages restricted to bands in granular carbonate rock. These bands are similar in appearance to the hausmannite ore layers, although hausmannite has not been found directly associated with plumboferrite (Flink, 1910).

The samples were studied in polished sections or polished thin sections. They generally show little mineralogical or textural variations. Plumboferrite always occurs in intimate association with hematite and spinel *sensu lato* (grain size 0.1–2.0 mm) and frequently with lindqvistite. Hematite is mainly a primary phase but also appears as a replacement product of both plumboferrite and spinel along cracks and grain boundaries. The oxide minerals usually display contacts toward patches of calcite. Andradite garnet and phlogopite mica are the only primary silicates found. Garnet occurs as euhedral grains that are on average 0.4 mm across, often with inclusions of the above oxides. Mica is occasionally subjected to incipient chloritization. Native copper and its alteration products (e.g., cuprite) also frequently follow plumboferrite. Barite and V-bearing svabite and hedyphane were detected as subordinate constituents of some of the samples investigated. Hematophanite, Pb₁Fe₃+O₃Cl, was found on one specimen (no. 280186) and has suffered to a large extent from secondary alteration and decomposed to goethite and hydrocerussite.

Igelström (1894) reported a second occurrence of plumboferrite from the mine Sjögruvan, Örebro, central Sweden. We reinvestigated the material from Sjögruvan, labeled by Igelström, but no traces of plumboferrite were detected. Thus, apart from finds in oxidized mine waste (Schnorrer-Köhler, 1986), no occurrence of the mineral other than at the type locality has been verified.

TABLE 2. Compositional data for spinels associated with plumboferrite

| Sample | 81:0224 | 280186 | 331072 | 670322 | 920741 | g7776 |
|--------------------------------|---------|--------|--------|--------|--------|-------|
| Oxide wt% | | | | | | |
| ZnO | 0.11 | 0.04 | 0.26 | 0.00 | 0.48 | 0.43 |
| FeO* | 8.36 | 8.87 | 6.88 | 8.12 | 8.70 | 7.56 |
| Fe ₂ O ₃ | 73.43 | 72.98 | 70.65 | 74.85 | 71.81 | 73.90 |
| MnO | 7.74 | 9.53 | 16.26 | 3.11 | 12.98 | 8.12 |
| TiO ₂ | 0.00 | 0.00 | 0.04 | 0.01 | 0.00 | 0.00 |
| Al ₂ O ₃ | 0.00 | 0.08 | 0.06 | 0.01 | 0.02 | 0.05 |
| MgO | 9.38 | 7.94 | 4.68 | 12.65 | 5.66 | 9.60 |
| Total | 99.02 | 99.44 | 98.83 | 98.75 | 99.65 | 99.68 |
| End-member mol% | | | | | | |
| Jac | 24 | 29 | 52 | 9 | 41 | 25 |
| Mag | 25 | 27 | 21 | 24 | 27 | 23 |
| Mgf | 51 | 44 | 26 | 67 | 31 | 51 |
| Fra | 0 | 0 | 1 | 0 | 1 | 1 |

Note: Jac = jacobsonite, Mag = magnetite, Mgf = magnesioferrite, Fra = franklinite.

* Fe²⁺ calculated assuming four O atoms per three cations.

CHEMICAL COMPOSITION

The chemical composition of the samples was obtained by electron microprobe (EMP) analysis, using a Cameca SX50 instrument maintained by Uppsala University and operated at 20 kV and 12 nA. Standards used and spectral lines measured have been given in an earlier paper (Holtstam and Norrestam, 1993). The PAP correction routine (Pouchou and Pichoir, 1984) was used for data reduction. The number of point analyses ranged from five to 30 for the different samples, and average analytical results are reported in Table 1. The concentrations of Ba, Zn, Cr, and Ca were at or below the detection limit in all cases. The compositions of several coexisting phases were also determined, and selected analyses of the spinel-type minerals are reported in Table 2. The material used by Igelström (1881) for his wet-chemical analysis of plumboferrite was afflicted with impurities, as indicated by a high CaO content. More reliable data were given by Johansson (1928).

No intragranular chemical heterogeneities were detected on back-scattered electron (BSE) images of plumboferrite. The intersample compositional variations are moderate (Table 1). The ratio between Pb and the smaller cations appears to be constant within the analytical uncertainty limits, estimated at $\pm 2\%$ (relative) for major oxides. Mn varies inversely with Mg, and the content of both metals tends to increase when the Ti content increases. These correlations suggest that the substitution mechanisms $Mg^{2+} \rightleftharpoons Mn^{2+}$ and coupled $(Mn,Mg)^{2+} + Ti^{4+} \rightleftharpoons 2Fe^{3+}$ operate in the mineral. The role of Fe²⁺ in plumboferrite is unclear. Wet-chemical analyses show 0.78 wt% FeO (Johansson, 1928), corresponding to an Fe²⁺/Fe_{tot} ratio of only 0.014. The O content of the present samples, as estimated by charge balance (Table 1), shows a remarkable consistency, which indicates that there exists no large variation in the Fe²⁺-Fe³⁺ ratio of plumboferrite.

Associated spinels (Table 2) essentially belong to the ternary system $(\text{Mg}, \text{Mn}, \text{Fe}^{2+})\text{Fe}_2\text{O}_4$. Spinel compositions are plotted in Figure 1, with the mineral assemblages indicated. Hematite is generally close to Fe_2O_3 in composition; maximum impurity contents are 0.09 wt% MnO, 0.32 wt% TiO_2 , and 0.18 wt% MgO.

PHYSICAL AND OPTICAL PROPERTIES

Plumboferrite is black with a submetallic luster. The streak is almost black; the reddish color reported by Igelström (1881) was probably due to hematite contamination in his powder sample. The crystals have a tabular habit and may reach a size of 10 mm across. The dominant forms are $\{0001\}$ and $\{10\bar{1}1\}$; cleavage is perfect parallel to (0001) .

Hardness measurements, using a Shimadzu type-M microhardness tester loaded with a 100 g weight, gave $VHN = 882$ (range 824–946 for ten measurements). The indentations were close to perfect and accompanied by radial fractures. Criddle and Stanley (1993) report a VHN_{100} of 926 for plumboferrite; both data sets correspond to a Mohs hardness of about 6.5. Igelström (1881) gave $H = 5$, a value obviously too low even if the anisotropy of the hardness, to be expected for a layer structure like that of plumboferrite, is considered.

The calculated density for no. 81:0224 is 6.093(2) g/cm^3 (from single-crystal refinements) or 6.12(1) g/cm^3 (from the microprobe analyses and powder data). Johansson (1928) reported a measured value of 6.07 g/cm^3 for his specimen. Plumboferrite is nonmagnetic; it is slowly attacked by cold hydrochloric acid, producing a yellowish solution, but it is unaffected by other common acids.

In reflected, linearly polarized light, plumboferrite is light gray, nonpleochroic, and only weakly birefractant. The mineral is opaque and lacks internal reflections and visible twinning. Reflectance measurements were made within the visible spectrum, using a Zeiss MPM800 photometer system equipped with a $10\times/0.20$ Ultrafluar objective and adjusted to give a field of measurement with a diameter of 40 μm . An SiC mount provided by Carl Zeiss Ltd., Oberkochen, was used as a standard. The values (R_o - R_e , in percent) obtained in air and reported for the four COM wavelengths are 25.6–24.2 (470 nm), 24.5–23.5 (546 nm), 23.7–22.8 (589 nm), and 22.6–22.1 (650 nm). Criddle and Stanley (1993) gave similar values, the greatest difference for the upper reflectance curve being 0.8% absolute (at 400 nm). Note that the values for R_o and R_e apparently were interchanged in Criddle and Stanley (1993), thus indicating an optically positive mineral. Our data are in agreement with those of Cameron (1963), who states that plumboferrite is uniaxial negative.

Plumboferrite is macroscopically very similar in appearance to the lead ferrite lindqvistite (Holtstam and Norrestam, 1993), and X-ray diffraction data, chemical analysis, or accurate reflectance measurements are needed to distinguish between the two minerals.

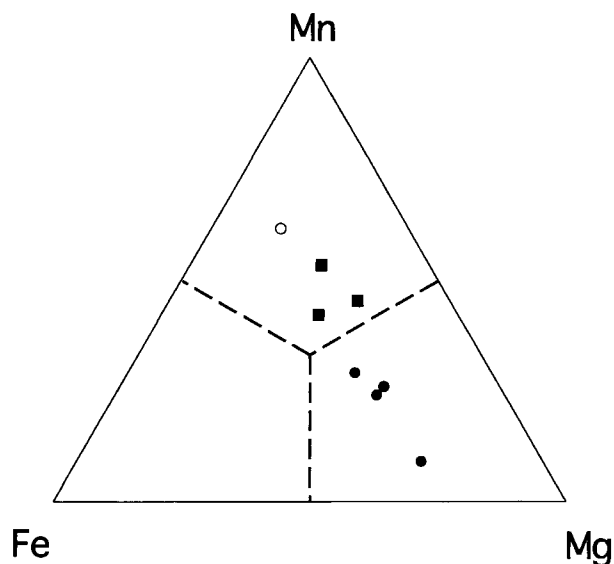


Fig. 1. Triangular plot of the system $(\text{Mg}, \text{Mn}, \text{Fe}^{2+})\text{Fe}_2\text{O}_4$ showing the composition of spinels. Solid circles, squares, and the open circle refer to pure plumboferrite samples, plumboferrite-lindqvistite pairs, and pure lindqvistite samples, respectively. Two of the data points are taken from Holtstam and Norrestam (1993); the others are from this work.

X-RAY CRYSTALLOGRAPHY

Single-crystal X-ray photography

Precession X-ray photographs of plumboferrite indicate a hexagonal unit cell, with the dimensions as given below. The systematically extinct intensities are consistent with the space-group symmetries $P6_3/mmc$, $P6_3/mc$, and $P\bar{6}2c$. Overexposed photographs taken at levels along $[0001]$ show weak extra reflections that could be indexed on a hexagonal unit cell three times larger. Also, some very weak and diffuse reflections along c^* indicate a tripling of the c dimension. The new, $9\times$ larger cell is obtained by the transformation matrix:

$$T_a = \begin{bmatrix} 2 & 1 & 0 \\ -1 & 1 & 0 \\ 0 & 0 & 3 \end{bmatrix}.$$

The hexagonal parameters for the supercell thus become $a' = \sqrt{3}a = 10.27 \text{ \AA}$ and $c' = 3c = 70.7 \text{ \AA}$. The results are consistent with those of Kohn et al. (1968), and similar superlattice reflections were also observed by Bovin (1981) in electron diffraction patterns of plumboferrite.

Powder diffraction

Accurate powder X-ray diffraction data for two of the samples were obtained using an automated diffractometer. They were collected at room temperature in the 2θ range 3–70°, with a step width and counting time of 0.01° and 2.5 s, respectively. Peak positions were adjusted against an external Si standard (SRM 640). Data for no. 81:0224, including intensities measured as relative peak

TABLE 3. X-ray powder diffraction data for plumboferrite

| l_{meas} | l_{calc} | d_{meas} (Å) | d_{calc} (Å) | hkl |
|-------------------|-------------------|-----------------------|-----------------------|--------|
| 40 | 49 | 11.78 | 11.77 | 002 |
| 25 | 11 | 5.888 | 5.887 | 004 |
| 5 | 8 | 5.132 | 5.136 | 100 |
| 6 | 15 | 5.024 | 5.018 | 101 |
| 85 | 24 | 3.922 | 3.925 | 006 |
| 4 | 6 | 3.469 | 3.471 | 105 |
| 8 | 13 | 3.118 | 3.119 | 106 |
| 12 | 52 | 2.9662 | 2.9653 | 110 |
| 100 | 22 | 2.9438 | 2.9437 | 008 |
| 7 | 23 | 2.8745 | 2.8755 | 112 |
| 30 | 73 | 2.8132 | 2.8142 | 107 |
| 30 | 100 | 2.6473 | 2.6484 | 114 |
| 9 | 16 | 2.5536 | 2.5541 | 108 |
| 10 | 6 | 2.5077 | 2.5091 | 202 |
| 15 | 31 | 2.4392 | 2.4407 | 203 |
| 9 | 3 | 2.3545 | 2.3549 | 0,0,10 |
| 4 | 18 | 2.2542 | 2.2547 | 205 |
| 2 | 5 | 2.1495 | 2.1489 | 206 |
| 2 | 8 | 2.0886 | 2.0891 | 118 |
| 3 | 4 | 1.9759 | 1.9761 | 1,0,11 |
| 4 | 2 | 1.9628 | 1.9625 | 0,0,12 |
| 6 | 10 | 1.8440 | 1.8442 | 1,1,10 |
| 6 | 5 | 1.8328 | 1.8328 | 209 |
| 7 | 6 | 1.7361 | 1.7357 | 2,0,10 |
| 3 | 5 | 1.7122 | 1.7120 | 300 |
| 16 | 8 | 1.6819 | 1.6821 | 0,0,14 |
| | 22 | | 1.6814 | 217 |
| 11 | 24 | 1.6442 | 1.6444 | 2,0,11 |
| | 13 | | 1.6439 | 304 |
| 4 | 9 | 1.6369 | 1.6365 | 1,1,12 |
| 5 | 9 | 1.6206 | 1.6206 | 218 |
| 10 | 26 | 1.4827 | 1.4827 | 220 |
| 4 | 5 | 1.4075 | 1.4072 | 2,0,14 |

Note: Philips PW1710 diffractometer, $\text{CuK}\alpha$ radiation.

heights above background, were indexed in accordance with the possible space-group symmetries (Table 3). To estimate the effect of preferred orientation of the crystallites, which enhances $00l$ reflections in the present case, intensities calculated from structural data were also included. The figure of merit (Smith and Snyder, 1979) for the present data set is $F_{30} = 46(0.010,63)$.

The hexagonal unit-cell parameters, refined from all 30 reflections by the least-squares method, are $a = 5.931(1)$, $c = 23.551(2)$ Å, and $V = 717.4(2)$ Å³ for $Z = 2$. For sample no. 670322, $a = 5.927(1)$ and $c = 23.535(3)$ Å. This sample's smaller cell volume, 715.9(3) Å³, is consistent with its lower Mn/Mg ratio.

Crystal-structure analysis

A plumboferrite platelet from specimen no. 81:0224 was isolated for crystal-structure analysis. X-ray diffraction data were collected with a single-crystal diffractometer at the Arrhenius Laboratory, Stockholm University, and corrected for background, Lorentz, polarization, and absorption effects. Atomic X-ray scattering factors for neutral atoms were taken from the compilation in *International Tables for X-ray Crystallography* (Ibers and Hamilton, 1974). The refinements were performed using the SHELX-76 program package (Sheldrick, 1976). Further

TABLE 4. Experimental conditions for the crystal-structure analysis of plumboferrite

| | |
|---|---|
| Space group | $P6_3/mmc$ |
| Unit-cell dimensions (single crystal) | $a = 5.9356(4)$, $c = 23.576(2)$ Å |
| Unit-cell V | 719.3(1) Å ³ |
| Radiation | $\text{MoK}\alpha$ (rotating anode) |
| Wavelength, λ | 0.71073 Å |
| T | 293(1) K |
| Crystal shape | tabular |
| Crystal size | 24 × 60 × 80 μm |
| Diffractometer | Siemens P4/RA |
| Determination of unit cell | |
| No. of refl. | 13 |
| 2θ range | 13.7–27.7° |
| Intensity data collection | ω - θ scan |
| Maximum (sin θ)/ λ | 0.81 Å ⁻¹ |
| Range of h , k , and l | –1–9, –1–9, and –1–38 |
| Internal R (after abs. corr.) | 0.048 |
| No. of collected refl. | 2878 |
| No. of unique refl. | 678 |
| No. of observed refl. | 394 |
| Criterion for significance | $I > 5\sigma_I$ |
| Absorption correction | numerical integration |
| Linear absorption coeff. | 34.1 cm ⁻¹ |
| Transmission factor range | 0.11–0.46 |
| Structure refinement | full-matrix least squares |
| Minimization of | $\sum w(\Delta F)^2$ |
| Anisotropic thermal param. | Fe atoms |
| Isotropic thermal param. | Pb and O atoms |
| Number of refined param. | 32 |
| Weighting scheme | $(\sigma^2 + 0.0003 F ^2)^{-1}$ |
| Final R for obs. refl. | 0.039 |
| Final R_w for obs. refl. | 0.045 |
| Final R_w for all refl. | 0.058 |
| Final $(\Delta/\sigma)_{\text{max}}$ | <0.001 |
| Final $\Delta\rho_{\text{min}}$ and $\Delta\rho_{\text{max}}$ | –4.2 and 3.0 e ⁻ /Å ³ |

experimental details are summarized in Table 4. Observed and calculated structure factors are given in Table 5.¹

The structural parameters for magnetoplumbite (Moore et al., 1989) were used as a starting point in the refinements, which were carried out in the space group $P6_3/mmc$. From the chemical data it appears that plumboferrite has a Pb:Fe stoichiometric relation of 2:11 instead of the 1:12 relation found in magnetoplumbite, and this fact suggests that an extra Pb atom replaces an Fe atom in one of the metal positions of the magnetoplumbite structure. Considering the similar X-ray scattering powers of the first-row transition elements and the minor amount of light elements present in the specimen, we refined it as if it were a pure Pb-Fe oxysalt. Assuming 100% occupation at each metal position, but allowing the Pb:Fe ratios to vary, did not provide any statistically relevant indication of mixed metal contents in these positions. Allowing the occupancies of the O positions to vary during the final steps of refinement indicated that the O atom at the $6h$ position, labeled O3 and located in the disordered layer (cf. the following) at $z = 1/4$, had an occupancy factor of only 73(4)%. The results thus suggest that the composi-

¹ A copy of Table 5 may be ordered as Document AM-95-595 from the Business Office, Mineralogical Society of America, 1015 Eighteenth Street NW, Suite 601, Washington, DC 20036, U.S.A. Please remit \$5.00 in advance for the microfiche.

tion of plumboferrite is $\text{Pb}_2\text{Fe}_{11}\text{O}_{18.2(1)}$. However, although the R_w value decreased significantly as a result of the introduction of incomplete occupation, the relevance of the occupancy-factor value is somewhat limited because the O3 atoms are positionally disordered, and the formulation of adequate disorder models is by no means straightforward.

In the plumboferrite structure, there are two unique Pb sites, Pb1 and Pb2, ideally located at a $2d$ ($\frac{2}{3}, \frac{1}{3}, \frac{1}{4}$) and a $2b$ ($0, 0, \frac{1}{4}$) position, respectively. However, in a case like this when one determines the structure averaged over the whole crystal, Pb atoms could deviate significantly from their ideal positions. On average, Pb1 and Pb2 are describable, as a first approximation, by locating them in $6h$ ($x, 2x, \frac{1}{4}$) positions, each with $\frac{1}{3}$ occupancy. When viewed along $[0001]$, the Pb atoms are found in the corners of equilateral triangles (Fig. 2). For Pb1 the triangle side (Pb1-Pb1' distance) is 0.86 \AA , and for Pb2 it is 0.74 \AA . It should be noted that by refining Pb1 as vibrating anisotropically and located on the mirror plane at $z = \frac{1}{4}$ (and $\frac{3}{4}$), the displacement component U_{33} becomes very large, $0.0304(9) \text{ \AA}^2$, compared with the other components [$U_{11} = U_{22} = 0.0075(4) \text{ \AA}^2$]. This indicates that Pb1 might become positionally disordered by deviating from the mirror plane. Although less pronounced, the situation is similar for Pb2. Refinement of isotropic Pb1 and Pb2 atoms in point position $12k$ ($x, 2x, z$) results only in a slight increase of R_w (4.5% compared with 4.3%). The z coordinates become $0.2557(1)$ and $0.2526(2)$, and the isotropic displacement factors obtain reasonable values of $0.0080(4)$ and $0.0054(3) \text{ \AA}^2$ for Pb1 and Pb2, respectively, whereas the rest of the structural parameters remain largely unchanged. The deviation from $z = \frac{1}{4}$, by 0.14 and 0.06 \AA , respectively, is significant for both atoms ($>15\sigma$). In summary, the disorder of the Pb atoms is more pronounced in the xy plane than along $[0001]$, and Pb1 is the more disordered of the two. No significant indication suggesting further splitting of the Pb atoms from the $12k$ ($x, 2x, z$) point positions was found in the final $\Delta\rho$ map.

The O3 atom at the point position $6h$ ($x, 2x, \frac{1}{4}$) has a considerably higher displacement factor, $U_{\text{iso}} = 0.042(7) \text{ \AA}^2$, than the other O atoms, suggesting positional disorder for this atom as well. Anisotropic refinement gave physically unreasonable values for the U_{ij} parameters. As seen in Figure 2, the electron-density distribution around O3 is very uneven. A proper fit to a model of a vibrating O3 would obviously require a higher odd-order tensor for a proper description, which explains the poor results for a simple anisotropic (2nd-order) model. The quality of the data is probably not good enough to permit the use of more elaborate models for this Pb mineral. Thus, O3 was kept isotropic (with variable occupation) in the refinements. There are also indications of disorder for the Fe3 atom. The U_{33} value of $0.0336(17) \text{ \AA}^2$ is much larger than $U_{11} = U_{22} = 0.0035(6) \text{ \AA}^2$, suggesting some degree of mobility of Fe3 along $[0001]$. However, it is not easy to

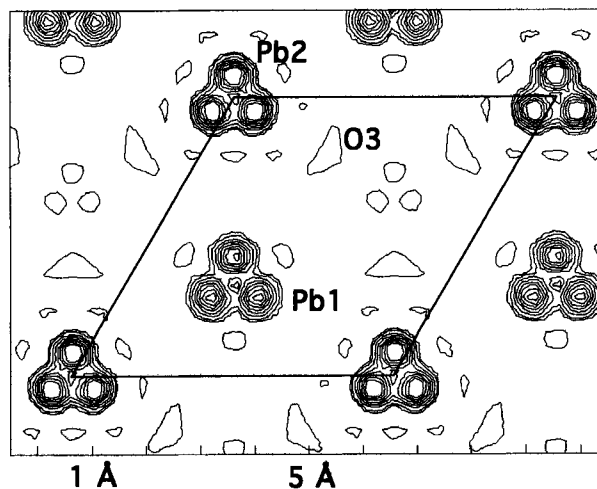


Fig. 2. Final electron-density map, $\rho(x, y, \frac{1}{4})$, for plumboferrite. The contours drawn correspond to 2, 4, 6, 10, 20, . . . , $80 \text{ e}^-/\text{\AA}^3$. The origin of the unit cell is at the upper left corner, with x downward and y horizontal.

formulate a simple disorder model for Fe3. One possibility is to locate a fraction of the Fe content exactly at the mirror plane at $z = \frac{1}{4}$ and position the other (mirror-related) fraction at $z = \frac{1}{4} \pm \zeta$, where $\zeta \approx 0.07$. Although this model would probably allow split isotropic Fe3 positions to be refined, the Fe3-O distances in the mirror plane would become too short to be reasonable.

For the finally adopted structural model the refinements converged to a conventional R index of 3.9% (weighted $R_w = 5.8\%$ for all reflections). The positional parameters and equivalent isotropic displacement factors for plumboferrite are given in Table 6, and bond lengths are shown in Table 7.

DISCUSSION

Crystal structure

The structure of plumboferrite (Fig. 3) is a derivative of the magnetoplumbite or M structure type, which in turn is a fundamental member of the prolific hexagonal ferrite family (Kohn et al., 1971; Collongues et al., 1990). It consists of a closest-packed ($chhhcchhhc$) ten-layer array of large atoms (O + Pb), with the smaller Fe atoms distributed over different interstitial sites. The basic building stones are the S and R blocks, which essentially have the structures of cubic spinel and hexagonal BaNiO_3 (Takeda et al., 1976), respectively. The M structure can be considered as a stacking sequence of such blocks along the hexagonal c axis, equal to RSR'S' for one unit cell (primed blocks are rotated π radians to comply with the space-group symmetry operations).

Pb1 is formally 12-fold ($8 + 4$) coordinated to O, whereas Pb2 is fivefold coordinated. There are five unique Fe sites in M, but the $^{57}\text{Fe}^{3+}$, ideally positioned at $(0, 0, \frac{1}{4})$,

TABLE 6. Occupancies, atom coordinates, and isotropic displacement parameters (\AA^2) for plumboferrite

| Atom | W | Occup. | x | y | z | U_{eq} |
|------|-----|---------|-------------|--------------|-------------|------------|
| Pb1 | 12k | 1/6 | 0.71470(16) | -0.71470(16) | 0.25575(10) | 0.0080(4) |
| Pb2 | 12k | 1/6 | 0.04168(13) | 0.08336(25) | 0.25265(17) | 0.0054(3) |
| Fe1 | 2a | 1 | 0 | 0 | 0 | 0.0042(7) |
| Fe2 | 4f | 1 | 1/3 | 2/3 | 0.02627(11) | 0.0037(5) |
| Fe3 | 4f | 1 | 1/3 | 2/3 | 0.18468(15) | 0.0135(7) |
| Fe4 | 12k | 1 | 0.16905(11) | 0.33810(22) | -0.10614(6) | 0.0041(3) |
| O1 | 4e | 1 | 0 | 0 | 0.1455(5) | 0.0047(20) |
| O2 | 4f | 1 | 1/3 | 2/3 | -0.0535(5) | 0.0037(19) |
| O3 | 6h | 0.73(5) | 0.1871(20) | 0.3743(40) | 1/4 | 0.0425(70) |
| O4 | 12k | 1 | 0.1566(6) | 0.3133(12) | 0.0515(3) | 0.0049(11) |
| O5 | 12k | 1 | 0.5031(6) | -0.5031(6) | 0.1482(3) | 0.0049(11) |

Note: W = Wyckoff notation of point position. The equivalent isotropic displacement parameters (U_{eq}) of the anisotropically refined Fe atoms were estimated as $1/3 \cdot \text{trace}(U)$. Estimated standard deviations of the last digits are given within parentheses.

is substituted by Pb^{2+} in plumboferrite. Despite the observed disorder and stoichiometric defects obviously related to this replacement, the remaining four sites have metal-O bond-distance averages similar to those of the true M-type compounds. Bond-valence sums for the different Fe positions were calculated using the empirical parameters of Brown and Altermatt (1985). For the octahedral sites the obtained values (in valence units) range between 2.8 and 3.0, and for the tetrahedral site the value is 2.7. Similar values are found for the corresponding sites in the structures of magnetoplumbite (Moore et al., 1989) and synthetic $\text{BaFe}_{12}\text{O}_{19}$ (Obradors et al., 1985). The largest differences are found, not unexpectedly, for the face-sharing Fe3 octahedra in the R blocks, which are most affected by disorder in the plane at $z = 1/4$.

The disorder of the two Pb atoms is similar to what has been observed in other Pb-bearing hexagonal ferrites. In synthetic magnetoplumbite, for example, the single, symmetry-independent Pb was found to be split over six

positions at $(x, y, 1/4)$, on the average $1/6$ occupied, and displaced 0.6 \AA from its ideal position at $2d$ ($2/3, 1/3, 1/4$). The phenomenon has been ascribed to the lone-pair effect (Moore et al., 1989). Pb^{2+} has a lone pair of electrons in its outermost shell, which in some cases is stereoactive and tends to push the central atom off center in its coordination polyhedron (Hyde and Andersson, 1989).

The partial occupancy for the O3 position is clearly related to a real O deficit, as indicated by the refined composition given above. O vacancies probably explain the (seemingly) unreasonably short Pb-O3 contacts (1.50 and 2.17 \AA) for Pb2 in plumboferrite and the unexpected disorder of the Fe3 atom; both have O3 ligands, and the X-ray data show only the average picture.

Superstructure and disorder

Because of the low quality and weak intensities of the superreflections mentioned above, it was not possible to collect and include them in the structural refinements. A few, speculative remarks can still be made about the causes of the observed pattern. A reasonable explanation for the $\sqrt{3}a$ repeat (Fig. 4) would be a tendency for the Pb atoms to order over the split positions in a two-dimensional superstructure. Because anion vacancies in a crystal structure are also likely to distribute themselves in an ordered fashion, due to repulsive forces, they might explain the superstructure indicated by the weak extra reflections along c^* .

The disorder model proposed here for the atoms in the central section of the R blocks of plumboferrite is very similar to that in lindqvistite (ideally given as $\text{Pb}_2\text{Me}^{2+}\text{Fe}_{16}\text{O}_{27}$), which has the stacking sequence RSSR'S'S' (Holtstam and Norrestam, 1993). Precession photographs of lindqvistite show the same superstructure reflections in a^*b^* . Although partial population of the O sites was not demonstrated, the empirical formulae indicate a slight deviation from stoichiometry in this compound also (Holtstam and Norrestam, 1993).

Like lindqvistite, plumboferrite undergoes structural changes and becomes magnetic upon heating in air. The powder XRD pattern of the heated material closely resembles that of magnetoplumbite (the change corresponds to a decrease in hexagonal cell volume by ca. 2%).

TABLE 7. The relevant metal-O distances (\AA) and multiplicities for the coordination polyhedra of plumboferrite

| Coordination | Bonds | Distance |
|--------------|-------------------|-----------|
| R_{6-4} | Pb1-O3 $\times 2$ | 2.585(16) |
| | -O5 $\times 2$ | 2.716(7) |
| | -O5' $\times 2$ | 2.946(7) |
| | -O3' $\times 2$ | 2.985(16) |
| | -O5'' $\times 1$ | 3.141(7) |
| | -O5''' $\times 1$ | 3.342(7) |
| R_5 | Pb2-O3 $\times 1$ | 3.429(16) |
| | -O3' $\times 2$ | 1.497(16) |
| | -O1 $\times 1$ | 2.171(16) |
| | -O1' $\times 1$ | 2.439(8) |
| | -O1'' $\times 1$ | 2.563(8) |
| S_6 | Fe1-O4 $\times 6$ | 2.017(6) |
| S_4 | Fe2-O2 $\times 1$ | 1.880(8) |
| | -O4 $\times 3$ | 1.912(7) |
| R_6 | Fe3-O5 $\times 3$ | 1.946(7) |
| | -O3 $\times 3$ | 2.152(16) |
| | Fe4-O5 $\times 2$ | 1.956(7) |
| $(RS)_6$ | -O1 $\times 1$ | 1.971(8) |
| | -O2 $\times 1$ | 2.097(8) |
| | -O4 $\times 2$ | 2.116(6) |

Note: R and S denote coordination polyhedra within the two types of structural blocks of the plumboferrite structure. RS denotes a polyhedron common to adjacent R and S blocks. The subscripts are the coordination numbers of the metal positions.

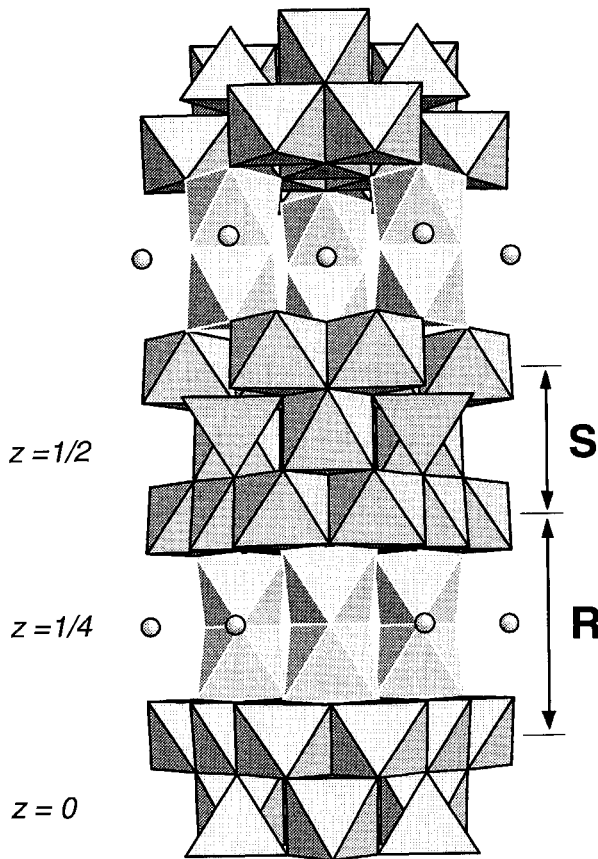


Fig. 3. Polyhedral representation of the plumboferrite structure, viewed approximately perpendicular to [0001]. The face-sharing octahedra around $z = 1/4$ are drawn with white edges. The structural entities defining the R and S blocks are indicated. The Pb atoms, located in the central section of the R block, are shown as spheres in their ideal positions. O vacancies are not considered in the drawing.

EMP analyses give 22.7 wt% PbO on average. The rate of change is very low; after 10 d only the outermost 50 μm of the crystals are affected, so the present experiments were conducted on powders. A reasonable explanation for this behavior is that a fraction of the Pb ions are transported out of the crystal during heating, but the exact nature of this process is unknown. It is not clear whether it causes crystal breakdown (and recrystallization to magnetoplumbite), or if the atom framework remains largely intact. Plumboferrite has a higher thermal stability than lindqvistite; the transformation is observed only at $T \geq 940^\circ\text{C}$, whereas lindqvistite is affected at $T \leq 840^\circ\text{C}$. Mountvala and Ravitz (1962) noted a strong endothermic peak around 950°C for PbFe_4O_7 but no corresponding exothermic peak during cooling.

The well-known solid electrolyte sodium β -alumina (e.g., Collongues et al., 1979), ideally $\text{NaAl}_{11}\text{O}_{17}$ (but often with excess Na and O), is a close cousin of the hexagonal ferrites. In this compound electric conduction results from the motions of Na^+ through the R blocks, i.e.,

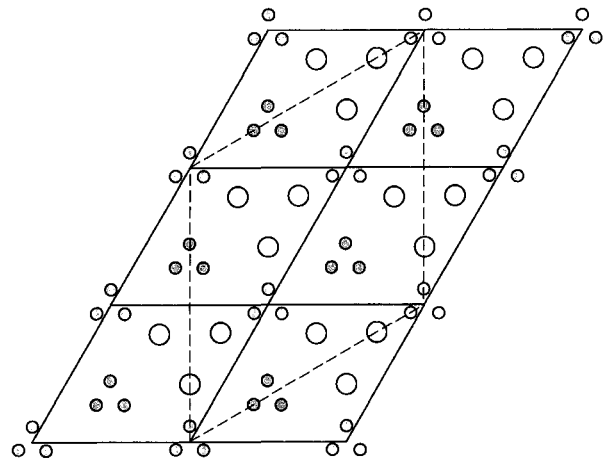


Fig. 4. Projection along [0001] showing the disordered layer at $z \approx 1/4$ in the plumboferrite structure. The split Pb positions are shown as shaded circles. The ideal O3 positions are shown by larger, open circles. Both the ordinary unit cell and the supercell with $a' = \sqrt{3}a$ (dashed line) are outlined.

β -alumina is a two-dimensional ionic conductor. If similar motions are active in the lead ferrites under heat treatment, a charge-compensating mechanism is needed. Two possibilities are oxidation of other cations (e.g., $\text{Mn}^{2+} \rightarrow \text{Mn}^{3+}$) and the creation of additional O vacancies.

Structural formula

A general structural formula for plumboferrite is $\text{Pb}(\text{PbFe}_{11})_{212}\text{O}_{19-3}\square_6$, where \square denotes a vacancy. A single O vacancy in two out of three R blocks corresponds to 18.33 O per half unit cell, which is in accord with the present structural and chemical analyses of plumboferrite. Such a scheme is also consistent with a c unit-cell dimension equal to three times that of the subcell. For charge balance it requires 0.33 formula units of a divalent cation (Me^{2+}) together with the Pb^{2+} and Fe^{3+} , yielding the expression $\text{Pb}_2(\text{Me}_{0.33}\text{Fe}_{10.67})\text{O}_{18.33}$, with $Z = 2$ for the subcell. Different formulations are possible when considering the content of the supercell, but we prefer to use an expression that shows the relation to the M-type compounds more clearly and emphasizes the defect nature of the phase. For natural plumboferrite, $\text{Me} = \text{Mn}^{2+}$ and Mg , but these elements cannot be considered essential for the mineral. A phase corresponding to plumboferrite was synthesized in the pure Pb-Fe-O system (Mountvala and Ravitz, 1962; Mexmain and Hivert, 1978), and its stabilization was probably achieved through the presence of small amounts of Fe^{2+} or by the accommodation of a greater number of O atoms in the structure. The close structural relationship between magnetoplumbite and plumboferrite suggests that the latter should be counted as a member of the magnetoplumbite group, despite the defects.

Paragenesis

The oxide mineral assemblage with plumboferrite as an essential component can be inferred to have formed

during maximum P - T conditions at Jakobsberg, whereas the appearance of native copper and secondary hematite and the breakdown of hematophanite are probably the results of later hydrothermal activity. The present mineral association gives few clues to the conditions of formation of plumboferrite. The presence of nearly pure andradite (≥ 98 mol% $\text{Ca}_3\text{Fe}_2\text{Si}_3\text{O}_{12}$) indicates f_{O_2} levels at least above the NNO buffer (Deer et al., 1982). On the other hand, there is no evidence of Mn^{3+} in the oxides present.

Three hexagonal lead ferrites are known in nature: magnetoplumbite, plumboferrite, and lindqvistite. The general prerequisites for their formation include relatively high f_{O_2} values and low activities of Si and S. There is indication that the crystallization of magnetoplumbite is favored by the coupled incorporation of Mn^{2+} and Ti^{4+} (Holtstam, 1994). Because the number of O vacancies is likely to increase with decreasing f_{O_2} , plumboferrite is probably favored by more reducing conditions relative to magnetoplumbite. The common coexistence of plumboferrite and lindqvistite suggests that they have similar stability limits. Obviously, plumboferrite requires more Pb and lindqvistite more divalent cations. It should also be noted that the pure plumboferrite samples contain magnesioferrite, whereas the plumboferrite-lindqvistite pairs coexist with more Mn-rich varieties of spinel (Fig. 1). In summary, the divalent cations play a crucial role in stabilizing these two phases, and the present data also suggest that variations in Mn/Mg are of importance.

ACKNOWLEDGMENTS

This work was supported financially by the Swedish Natural Science Research Council (NFR). Comments by P.B. Moore and J.A. Kohn on the manuscript are gratefully acknowledged.

REFERENCES CITED

- Björk, L. (1986) Beskrivning till Berggrundskartan Filipstad NV. Sveriges Geologiska Undersökning, Af 147, 1–110.
- Bovin, J.-O. (1981) High resolution transmission electron microscopy of minerals: Defects and new combination structures in the högbomite group. *Geologiska Föreningens i Stockholm Förhandlingar*, 103, 122–124.
- Brown, I.D., and Altermatt, D. (1985) Bond-valence parameters obtained from a systematic analysis of the inorganic crystal structure database. *Acta Crystallographica*, B41, 244–247.
- Cameron, E.N. (1963) Optical symmetry from reflectivity measurements. *American Mineralogist*, 48, 1070–1079.
- Collongues, R., Kahn, A., and Michel, D. (1979) Superionic conducting oxides. *Annual Review of Materials Science*, 9, 123–150.
- Collongues, R., Gourier, D., Kahn-Harari, A., Lejus, A.M., Théry, J., and Vivien, D. (1990) Magnetoplumbite-related oxides. *Annual Review of Materials Science*, 20, 51–82.
- Criddle, A.J., and Stanley, C.J. (1993) Quantitative data file for ore minerals (3rd edition), 698 p. Chapman and Hall, London.
- Deer, W.A., Howie, R.A., and Zussman, J. (1982) Rock-forming minerals, vol. 1A: Orthosilicates (2nd edition), 919 p. Longman, London.
- Fleischer, M., and Mandarino, J.A. (1991) Glossary of mineral species, 256 p. Mineralogical Record, Tucson, Arizona.
- Flink, G. (1910) Bidrag till Sveriges mineralogi II. *Arkiv för Kemie Mineralogi och Geologi*, 3(35), 1–166.
- Holtstam, D. (1994) Mineral chemistry and parageneses of magnetoplumbite from the Filipstad district, Sweden. *European Journal of Mineralogy*, 6, 711–724.
- Holtstam, D., and Norrestam, R. (1993) Lindqvistite, $\text{Pb}_2\text{Me}^{2+}\text{Fe}_{16}\text{O}_{27}$, a novel hexagonal ferrite mineral from Jakobsberg, Filipstad, Sweden. *American Mineralogist*, 78, 1304–1312.
- Hyde, B.G., and Andersson, S. (1989) *Inorganic crystal structures*, 432 p. Wiley, New York.
- Ibers, J.A., and Hamilton, W.C., Eds. (1974) *International tables for X-ray crystallography*, vol. IV, 366 p. Kynoch, Birmingham, U.K.
- Igelström, L.J. (1881) Plumboferrit, ett nytt mineral från Jakobsbergs manganmalmsgrufva vid Nordmarken i Wermland. Öfversigt af Kongliga Vetenskaps-Akademiens Förhandlingar, 38, 27–31.
- (1894) Mineralogiska meddelanden: 21. Plumboferrit från Sjögrufvan, Grythytte Socken, Örebro län. *Geologiska Föreningens i Stockholm Förhandlingar*, 16, 594–596.
- Johansson, K. (1928) Mineralogische Mitteilungen: 2. Über Zusammensetzung und Kristallographie des Plumboferrits. *Zeitschrift für Kristallographie*, 68, 91–102.
- Kohn, J.A., Peacor, D.R., and Eckart, D.W. (1968) Plumboferrite: Cell, symmetry, and basic structure. *Geological Society of America Abstracts with Programs*, 162–163.
- Kohn, J.A., Eckart, D.W., and Cook, C.F. (1971) Crystallography of the hexagonal ferrites. *Science*, 172, 519–525.
- Magnusson, N.H. (1929) Nordmarks malmtrakt. *Sveriges Geologiska Undersökning*, Ca 13, 1–98.
- Mexmain, J., and Hivert, S.-L. (1978) Préparation et caractérisation de ferrites de plomb. *Annales de Chimie (science de matériaux)*, 3, 91–97.
- Moore, P.B. (1970) Mineralogy and chemistry of Långban-type deposits in Bergslagen, Sweden. *Mineralogical Record*, 1, 154–172.
- Moore, P.B., Sen Gupta, P.K., and Le Page, Y. (1989) Magnetoplumbite, $\text{Pb}^{2+}\text{Fe}_{17}^{2+}\text{O}_{19}$: Refinement and lone-pair splitting. *American Mineralogist*, 74, 1186–1194.
- Mountvala, A.J., and Ravitz, S.F. (1962) Phase relations and structures in the system $\text{PbO-Fe}_2\text{O}_3$. *Journal of the American Ceramic Society*, 45, 285–288.
- Obradors, X., Collomb, A., Pernet, M., Samaras, D., and Joubert, J.C. (1985) X-ray analysis of the structural and dynamic properties of $\text{BaFe}_{12}\text{O}_{19}$ hexagonal ferrite at room temperature. *Journal of Solid State Chemistry*, 56, 171–181.
- Pouchou, J.L., and Pichoir, F. (1984) A new model for quantitative X-ray microanalysis: I. Application to the analysis of homogeneous samples. *La Recherche Aérospatiale*, 3, 13–36.
- Schnorrer-Köhler, G. (1986) Neue Minerale von der Schlackenhalde der ehemaligen Zinkhütte Genna in Letmathe/Sauerland. *Der Aufschluss*, 37, 55–67.
- Sheldrick, G.M. (1976) SHELX-76: Program for crystal structure determination. University of Göttingen, Göttingen, Germany.
- Smith, G.S., and Snyder, R.L. (1979) F_N : A criterion for rating powder diffraction patterns and evaluating the reliability of powder-pattern indexing. *Journal of Applied Crystallography*, 12, 60–65.
- Takeda, Y., Kanamaru, F., Shimada, M., and Koizumi, M. (1976) The crystal structure of BaNiO_3 . *Acta Crystallographica*, 32, 2464–2466.

MANUSCRIPT RECEIVED JANUARY 3, 1995

MANUSCRIPT ACCEPTED MAY 9, 1995